Gaining efficiency by parallel quantification and identification of iTRAQ-labeled peptides using HCD and decision tree guided CID/ETD on an LTQ Orbitrap†

Nikolai Mischerikow,[ab] Pim van Nierop,[c] Ka Wan Li,[c] Hans-Gert Bernstein,[d] August B. Smit,[c] Albert J. R. Heck*[abe] and A. F. Maarten Altelaar*[ab]

Received 26th April 2010, Accepted 5th July 2010
DOI: 10.1039/c0an00267d

Isobaric stable isotope labeling of peptides using iTRAQ is an important method for MS based quantitative proteomics. Traditionally, quantitative analysis of iTRAQ labeled peptides has been confined to beam-type instruments because of the weak detection capabilities of ion traps for low mass ions. Recent technical advances in fragmentation techniques on linear ion traps and the hybrid linear ion trap-orbitrap allow circumventing this limitation. Namely, PQD and HCD facilitate iTRAQ analysis on these instrument types. Here we report a method for iTRAQ-based relative quantification on the ETD enabled LTQ Orbitrap XL, which is based on parallel peptide quantification and peptide identification. iTRAQ reporter ion generation is performed by HCD, while CID and ETD provide peptide identification data in parallel in the LTQ ion trap. This approach circumvents problems accompanying iTRAQ reporter ion generation with ETD and allows quantitative, decision tree-based CID/ETD experiments. Furthermore, the use of HCD solely for iTRAQ reporter ion read out significantly reduces the number of ions needed to obtain informative spectra, which significantly reduces the analysis time. Finally, we show that integration of this method, both with existing CID and ETD methods as well as with existing iTRAQ data analysis workflows, is simple to realize. By applying our approach to the analysis of the synapse proteome from human brain biopsies, we demonstrate that it outperforms a latest generation MALDI TOF/TOF instrument, with improvements in both peptide and protein identification and quantification. Conclusively, our work shows how HCD, CID and ETD can be beneficially combined to enable iTRAQ-based quantification on an ETD-enabled LTQ Orbitrap XL.

Introduction

The relative quantitative comparison of differences in peptide and protein abundances, between two or more samples, has become an important experiment type in MS-based biological and medical research.[1,2] For this purpose, numerous analytical strategies have been devised that are based on the incorporation of stable heavy isotopes into proteins or peptides of one sample, which is then mixed and analyzed in parallel with a sample labeled with light isotopes so as to provide internal reference to one another. Both metabolic labeling of proteins, such as ^{15}N-labeling and SILAC, whereby stable isotopes are incorporated in cell culture[3] or in the whole organism,[4–7] as well as chemical labeling of peptides after digestion, such as ICAT,[8] iTRAQ[9] or dimethylation labeling,[10,11] are frequently used. Of these, the fully MS/MS-based iTRAQ quantification strategy allows between 4- and 8-fold multiplexing, which is not easily achieved by any other method, making it a popular application particularly in clinical proteomics. Quantification by iTRAQ differs from other quantitative proteomics approaches, which are based on precursor ion intensities, by the production of iTRAQ specific reporter ions after MS/MS fragmentation. The iTRAQ labels are isobaric as they consist of a reporter and a balance moiety, which together result in an equal mass for every label. Peptides from multiple samples are differentially labeled and are selected for MS/MS as a single precursor ion. Upon fragmentation by CID, 4–8 specific reporter ions are released and used for quantification. Advantages of the iTRAQ strategy are beneficial signal intensity on the MS level, as the label is isobaric, as well as good quantification accuracy due to low sample noise on the MS/MS level.

From the analytical perspective, iTRAQ is traditionally performed on beam type rather than trapping type mass spectrometers. The latter instruments cannot trap iTRAQ reporter ions generated during MS/MS of typical proteolytic peptides (600–800 *m*/*z* with 2–3 charges) because the voltage commonly applied for optimal resonant excitation of the precursor shifts the

[a]*Biomolecular Mass Spectrometry and Proteomics Group, Bijvoet Centre for Biomolecular Research and Utrecht Institute for Pharmaceutical Sciences, Utrecht University, Padualaan 8, 3584 CH Utrecht, The Netherlands. E-mail: a.j.r.heck@uu.nl; m.altelaar@uu.nl; Fax: +31 30 2536919; Tel: +31 30 253 9554; +31 30 253 6797*
[b]*Netherlands Proteomics Centre, Padualaan 8, 3584 CH Utrecht, The Netherlands*
[c]*Department of Molecular and Cellular Neurobiology, Center for Neurogenomics and Cognitive Research, VU University Amsterdam, De Boelelaan 1085, 1081 HV Amsterdam, The Netherlands*
[d]*Department of Psychiatry, University of Magdeburg, Leipziger Strasse 44, 39120 Magdeburg, Germany*
[e]*Centre for Biomedical Genetics, Padualaan 8, 3584 CH Utrecht, The Netherlands*

† Electronic supplementary information (ESI) available: Supplementary table. See DOI: 10.1039/c0an00267d

low *m*/*z* fragments, including the iTRAQ reporter ions, beyond the stability limit, resulting in ejection from the trap. However, two technical developments offer the possibility to do iTRAQ on an ion trap instrument. One is the implementation of PQD[12] on the LTQ linear ion trap and the hybrid LTQ Orbitrap[13] to overcome the detection limit for low mass ions posed by regular resonant CID. PQD is an alternative fragmentation method to CID in linear ion traps allowing low *m*/*z* fragment ions to be trapped.[14] A more recent technical advance, which lifts this limitation in a different way, is the implementation of HCD on the LTQ Orbitrap. HCD allows MS/MS fragmentation 'in space' in a dedicated collision cell comparable to Q-TOF like precursor fragmentation.[15]

The applicability of both PQD and HCD for iTRAQ-based quantification has been the subject of several recent studies. Griffin *et al.*[16] showed that PQD on an LTQ performs comparable to CID on the QSTAR hybrid quadrupole TOF instrument with respect to quantification performance. Bantscheff *et al.*[17] described the implementation of PQD on an LTQ Orbitrap for the purpose of iTRAQ analysis, and showed that it outperforms the Q-TOf Ultima quadrupole TOF instrument in number of quantified proteins. They also showed that PQD is faster and more sensitive than HCD on an LTQ Orbitrap equipped with a prototype HCD cell. Another study by Zhang *et al.*[18] demonstrated that iTRAQ labeled phosphorylated peptides can be analyzed quantitatively by HCD on an LTQ orbitrap. In these studies, the need for optimization of PQD or HCD to yield both sequence-informative fragment ions and iTRAQ reporter ions in a single fragmentation event results in a compromise between optimal settings for identification and optimal settings for quantification. Although in the above studies HCD and PQD methods were able to outperform older generation TOF instruments, recent studies showed that PQD and HCD are significantly slower, less sensitive and produce less informative fragment ion spectra than CID analysis on current ion trap instruments.[19–21] Therefore, an alternative strategy was developed combining quantification by HCD with identification using CID.[19,21]

Recently, electron transfer dissociation (ETD) of peptides was introduced as an alternative peptide fragmentation method.[22,23] In ETD, the interaction between (near-) thermal electrons and positively charged peptides results in dissociation of the peptide N–C_α bond, producing c'-and z-type ions. Since ETD prefers larger and more basic peptides, which attain multiple charges during ESI, as compared to CID, the two techniques are considered largely complementary.[24,25] Reduced fragmentation efficiency of ETD for doubly charged peptides is compensated by the use of supplemental collisional activation (ETcaD).[26] With the implementation of ETD, two groups studied the dissociation of iTRAQ labeled peptides upon ETD. Both Han *et al.*[27] and Phanstiel *et al.*[28] found that the iTRAQ label does not release reporter ions as straightforward upon ETD as it does upon CID, which is caused by the difference in cleavage site within the iTRAQ label, amenable to either ETD or CID. Where in CID only unique reporter ions are observed after cleavage of the iTRAQ label, N–C_α cleavage upon ETD releases multiple fragment ions. Although unique iTRAQ reporters are observed with ETD, the high multiplexing capability of iTRAQ can only be used upon ETD followed by CID.[29] Circumventing these issues, a recent workflow by Yang *et al.*[30] described sequential PQD and ETD on an LTQ for the quantification of phosphorylated peptides, whereby both PQD and ETD contribute peptide sequence information but iTRAQ quantification is based on the PQD scan alone.

Here, we present a parallel acquisition setup which implements ETD for iTRAQ-based quantification on a HCD- and ETD-enabled LTQ Orbitrap XL. iTRAQ reporter ions are generated using HCD while sequence information is gathered in parallel using ETD or CID. The selection of ETD or CID is made on the fly according to the *m*/*z* of the precursor.[31] We demonstrate the performance of our workflow by the analysis of iTRAQ labeled peptides derived from synaptic preparations of human brain biopsies, and we show that in terms of identified and quantified peptides we outnumber the commercial 4800 Proteomics Analyzer MALDI TOF/TOF instrument, which has recently been shown to have equal performance as the modern ESI-Q-TOF platform QSTAR Elite.[32]

Our workflow requires only very little optimization, which is a benefit compared to the PQD-based approach, and allows on-the-fly, decision-tree-based CID/ETD analyses based on the physicochemical properties of the sampled peptides, since the same iTRAQ reporter ions are generated irrespective of CID or ETD precursor fragmentation. Furthermore, the low number of ions needed for the HCD generation of the iTRAQ reporter ions allows the experiment to be conducted on similar time scales as PQD or HCD alone. Our method leads to a significant gain in efficiency in protein quantification by conducting iTRAQ quantification in the HCD collision cell and proficient parallel identification using decision tree guided CID/ETD peptide fragmentation.

Experimental procedures

Preparation of BSA samples

500 μg BSA were solubilized in 100 μL 0.5 M triethylammonium bicarbonate at pH 8.5 with 10 μL 50 mM tris(2-carboxyethyl) phosphine. After incubation for 1 h at 55 °C, 5 μL 200 mM methylmethanethiosulfonate were added and vortexed for 10 min. Subsequently, trypsin was added (trypsin : protein 1 : 50) and incubated overnight at 37 °C. The sample was split into four equal aliquots, and isopropanol and 1 unit of iTRAQ 8-plex reagent were added (channels 113, 115, 117 and 119). After incubation for 2 h at room temperature, samples were centrifuged and the supernatant was dried in a vacuum centrifuge. BSA peptides labeled with 4 out of 8 iTRAQ 8-plex channels (113, 115, 117 or 119) were diluted to 10 fmol μL^{-1} and mixed in ratios 1 : 1 : 1 : 1, 1 : 1 : 2 : 4 or 2 : 2 : 3 : 4, with the lowest concentration being 20 fmol of labeled BSA injected on column.

Preparation of human brain samples

The research presented here was given written approval by the ethics commission of the University of Magdeburg, Germany. Samples from the left dorsolateral frontal cortex were obtained from four psychiatric healthy persons as described.[33] The specimens were collected at different times *postmortem* (12, 17, 21 and 22 hours), immediately frozen in liquid nitrogen, and stored at −80 °C until further processing. Isolation of synaptic membranes

from these brains as well as labeling with iTRAQ reagents was performed according to the same protocol used for the preparation of rodent samples.[34] In brief, synaptic membranes were solubilized in 30 μL of 0.85% (w/v) RapiGest (Waters). After reduction and alkylation of cysteine residues, the proteins were digested with trypsin overnight at 37 °C. The four peptide samples were tagged with 4 out of 8 iTRAQ 8-plex reagents (114, 116, 118 and 121), pooled, and then fractionated by SCX on a 2.1 × 150 mm polysulfoethyl A column (PolyLC) with a linear gradient of 0–500 mM KCl in 20% (v/v) acetonitrile and 10 mM KH_2PO_4 pH 2.9 over 25 min at a flow rate of 200 μL min^{-1}. SCX fractions were collected (36 in total) and further analyzed without further treatment by online LC-MS/MS or by offline LC separation followed by MS/MS.

RP-LC and MALDI TOF/TOF analysis

For the MALDI MS experiment SCX fractions were separated on an analytical capillary C18 column (150 mm × 100 μm ID) at 400 nL min^{-1}, using a linear increase in concentration of acetonitrile from 5 to 50% (v/v) in 90 min and to 90% in 10 min. The eluent was mixed with matrix (7 mg of re-crystallized α-cyano-hydroxycinnaminic acid in 1 mL 50% (v/v) acetonitrile, 0.1% (v/v) trifluoroacetic acid, and 10 mM ammonium dicitrate) delivered at a flow rate of 1.5 μL min^{-1}, deposited offline to a metal target (Applied Biosystems) every 15 seconds for a total of 384 spots. The sample was analyzed on an ABI 4800 Proteomics Analyzer (Applied Biosystems) and the data were processed as previously reported.[34]

RP-LC and analysis on the ETD-enabled LTQ Orbitrap

Analysis of SCX fractions was performed on an LC-coupled LTQ Orbitrap XL, equipped with an ETD reagent source (Thermo Fisher Scientific). An Agilent 1200 series HPLC system was equipped with a 20 mm Aqua C18 (Phenomenex) trapping column (100 μm ID, 5 μm particle size) and a 400 mm ReproSil-Pur C18-AQ (Dr Maisch GmbH) analytical column (50 μm ID, 3 μm particle size). Trapping was performed at 5 μL min^{-1} solvent A (0.1 M acetic acid in water) for 10 min, and elution was achieved with a gradient of 10 to 35% (v/v) solvent B (0.1 M acetic acid in 1 : 4 acetonitrile : water) in a total analysis time of 120 min. For analysis of BSA digests, the total analysis time was shortened to 45 min. During elution, the flow rate was passively split to 100 nL min^{-1}. Fused silica emitters (New Objective, 10 μm tip ID) biased to 1.7 kV were used for nano-electrospray. The LTQ Orbitrap was operated in data dependent mode to automatically switch between MS and MS/MS. MS spectra in the range of *m/z* 350–1500 were acquired in the orbitrap at a FWHM resolution of 30 000 after accumulation to an AGC target value of 500 000 in the linear ion trap with 1 microscan. The three most abundant precursor ions were selected for fragmentation by HCD followed by CID or ETD with an isolation width of 3 Th. If not stated differently, HCD was performed at 55% NCE in the dedicated collision cell at the back end of the C-trap, after accumulation to an AGC target value of 50 000 in the linear ion trap with 1 microscan, and fragments were read out in the orbitrap at a FWHM resolution of 7500, resulting in an average scan time of 0.7 s. CID and ETD were performed in the linear ion trap after accumulation to an AGC target value of 50 000 with 1 microscan (average total scan time 0.3 and 0.5 s, respectively). HCD and CID reaction time was set to 30 ms. The ETD reagent was fluoranthene which was accumulated in the ion trap to an AGC target value of 20 000. Charge state-dependent ETD reaction time was set to 50 ms for 2+ precursor ions, and supplemental activation[24] was used. The LTQ Orbitrap was set to automatically switch between CID and ETD, based on a combination of peptide *m/z* and charge state. In all experiments, fragmented precursors were dynamically excluded from further fragmentation for 30 seconds within a mass window of 60 ppm.

Data processing

In the case of LTQ Orbitrap XL data, raw files were processed with Proteome Discoverer 1.0 (Thermo Fisher Scientific) to extract separate DTA files for HCD, CID and ETD spectra. In the case of ETD fragment ion spectra, peaks resulting from non-fragmented precursor, charge-reduced precursors, and neutral losses from the charge-reduced precursor were automatically removed by the software. In the case of 4800 Proteomics Analyzer data, monoisotopic peak lists were extracted using TS2 Mascot software (Matrix Science) at a signal to noise level of 5. Peak lists from both instruments used for protein identification were filtered to include only the eighty most intense peaks prior to database searching. Database searches were performed using Mascot 2.2.1 (Matrix Science) licensed in-house. In the case of human samples, Mascot was setup to search the SwissProt database (version 56.2) with taxonomic restriction to *Homo sapiens* (20 407 sequences), using iTRAQ 8-plex as quantification mode and methionine oxidation as additional variable modification. In the case of BSA, the IPI bovine database (version 3.22 with 32 915 sequences) was searched. The mass tolerance of precursor ions was set to 5 ppm (for LTQ Orbitrap XL data) or 300 ppm (for 4800 Proteomics Analyzer data) and that of fragment ions to 0.6 Da. Up to 2 missed cleavages were allowed and trypsin was specified as enzyme. Peptide identifications were established at a significance of at least 0.01, resulting in false discovery rates of 2–3% for all three datasets, as reported by the Mascot search engine which uses a target-decoy strategy.

For subsequent data analysis, only peptides that uniquely map to one of the identified proteins in the experiment were included. Protein identification was based on the presence of two or more significant (ion score greater than or equal to homology threshold) unique peptides that map to a protein. iTRAQ reporter ion intensities were extracted from peak lists with a 0.2 Da (for 4800 Proteomics Analyzer data) or 0.006 Da (for LTQ Orbitrap XL data) mass window using custom software. HCD quantification data were associated to CID and ETD peptide annotations based on scan numbers provided by the instrument. Quantification data were corrected for iTRAQ isotope impurities, and label-specific bias was removed by log2-transformation of the data and subtraction of the mean reporter ion intensity of the respective label in the experiment. Finally, reporter intensities were standardized by expressing each relative to the mean reporter intensity within the spectrum. Differences in protein abundance were determined by comparing mean log2 reporter ion intensities of spectra associated with a particular protein, and

the significance was assessed using standard *t*-statistics. For a spectrum to be used for quantification it was required that every reporter ion could be measured, and that the highest reporter ion intensity in the spectrum exceeded 2000 (for 4800 Proteomics Analyzer data) or 5000 (for LTQ Orbitrap XL data). There was no requirement on the significance level of peptide annotation for spectra to contribute to protein quantification.

Results and discussion

To implement iTRAQ-based peptide quantification on an ETD- and HCD-enabled LTQ Orbitrap, we performed peptide quantification in parallel with peptide identification (Fig. 1A). Peptide identification was performed by the common combination of precise precursor *m*/*z* determination using the orbitrap analyzer and precursor sequencing by CID or ETD in the linear ion trap. For peptide quantification, the same precursors selected for fragmentation by CID or ETD were selected for fragmentation by HCD in the octopole collision cell, and fragment ions were analyzed in the orbitrap. For this purpose, the instrument was operated in data-dependent acquisition mode, whereby three HCD followed by three CID or ETD data-dependent MS/MS scans succeeded the MS scan. The HCD scans were relatively fast, because we set the instrument to an AGC target value of only 50 000 for HCD fragmentation, 4 to 6 times smaller than previously reported.[19,21] A higher AGC target value was not required because the HCD spectrum was only used to read out iTRAQ reporter ions and not to provide high quality fragment ion information. Furthermore, since in the orbitrap analyzer scan time increases proportionally with increasing resolution and resolution increases proportionally with decreasing *m*/*z*, HCD fragment ion read out with a FWHM resolution of 7500 at *m*/*z* 400 also reduced the scan time, while still obtaining a resolution of 16 000 at the iTRAQ reporter ions *m*/*z*. This high resolution read out is important to be able to resolve the iTRAQ reporters in the presence of possible interfering compounds.[35] The MS scan was acquired at 30 000 FWHM resolution, typically leading to scan times of around 750 milliseconds.

To assess our method in analytical terms, we analyzed three relatively simple peptide mixtures, namely tryptic BSA peptides labeled with 4 out of 8 iTRAQ 8-plex channels (113, 115, 117 or 119), mixed in ratios 1 : 1 : 1 : 1, 1 : 1 : 2 : 4 or 2 : 2 : 3 : 4. As our experimental setup is based on separate identification and quantification events, we did not have to tune the HCD event to yield balanced quantification and identification information from the HCD spectrum, but rather varied HCD collision energy to produce mainly iTRAQ reporter ions. For this purpose, we analyzed each of the three ratios at 35, 45, 55 and 65% NCE. All other parameters were held constant, including the AGC target value for HCD, which we set to 50 000 with a single microscan. HCD spectra were recorded in profile mode. For peptide identification in these experiments, we used CID.

A typical spectrum pair on the MS/MS level, consisting of a CID and a HCD spectrum, recorded for the BSA peptide LGEYGFQNALIVR, is shown in Fig. 1. While the CID spectrum (Fig. 1B) provides the expected b and y fragment ion series used for peptide identification, the HCD spectrum (Fig. 1C) contains almost solely iTRAQ reporter ions, resulting in confident and efficient quantification. All other spectra displayed similar characteristics, with the HCD spectra ideal for detecting iTRAQ reporter ions and the CID/ETD spectra ideal for parallel identification.

The analysis of the BSA LC-MS/MS runs, which are shown for ratios 1 : 1 : 1 : 1 and 1 : 1 : 2 : 4 in Fig. 2, demonstrates that the variation of collision energy has little or no influence on the relative variance of reporter ion intensities (Fig. 2A and B), which is measured as standard deviation of the normalized reporter ion intensities of all quantified peptides. The variance is around 10% for every iTRAQ channel, at all collision energies measured. These variances propagate into 10% uncertainty in reporter ion ratios (Fig. 2C and D as well as Fig. 2E and F), again independent of collision energy. Note that the measured mixing ratios deviate from the nominal mixing ratios of 1 : 1 : 1 : 1 (observed as 1 : 1.3 : 1.5 : 1.4) and 1 : 1 : 2 : 4 (observed as 1 : 1.2 : 3.1 : 6) due to differences in the concentration of iTRAQ-labeled preparations. When dividing experimental ratios displayed in Fig. 2F by the experimental ratios shown in Fig. 2E the ratios are 1 : 1 : 2 : 4, as expected. In a typical large scale quantitative proteomics experiment such as described in the next section, the influence of differences in overall peptide concentration between iTRAQ-labeled samples on the observed protein regulation is removed by a normalization procedure that has the critical assumption that the majority of proteins does not differ between samples.[34] Because BSA is the only protein, normalization was not applied in this experiment since this by definition would remove any observations of changes in BSA abundance.

What is affected by collision energy variation, though, is the number of quantified spectra (Fig. 2G and H). This number increases with collision energy, because the number of spectra that lack a reporter ion decreases. These spectra, although the other channels are present, were excluded from the quantification. At all ratios tested, 55% NCE during HCD resulted in the highest number of quantifiable spectra. In contrast, the number of identified spectra, as it is not based on the HCD event, did not change with collision energy.

To demonstrate that ETD can be easily integrated into our workflow, we also analyzed the BSA mixtures with the HCD CID/ETD method. For peptide identification we used either CID or ETD, whereby the fragmentation type was chosen for every single precursor according to the decision tree logic that was recently published by Swaney *et al.*[31] This logic is based on the observation that peptides with a charge greater than 2+ up to a certain *m*/*z* threshold are more likely to be identified from their ETD rather than their CID spectrum. For peptides above these *m*/*z* thresholds, and for all unmodified 2+ peptides, irrespective of their *m*/*z* value, CID provides better sequence information.[31,36] In comparison, both methods, HCD CID as well as HCD CID/ETD, performed comparably well on this simple peptide mixture (data not shown).

To test our methods in a biologically relevant experimental setting, we analyzed peptide mixtures generated by tryptic digestion of synaptic preparations of four *postmortem* human brain samples with both HCD CID and HCD CID/ETD. The four peptide mixtures were labeled with the 4 out of 8 iTRAQ 8-plex channels 114, 116, 118 and 121, pooled, and then pre-fractionated by SCX prior to MS analysis. Selected SCX fractions were analyzed by LC-MS/MS on the LTQ Orbitrap using the HCD CID and HCD CID/ETD method, and for a one-to-one

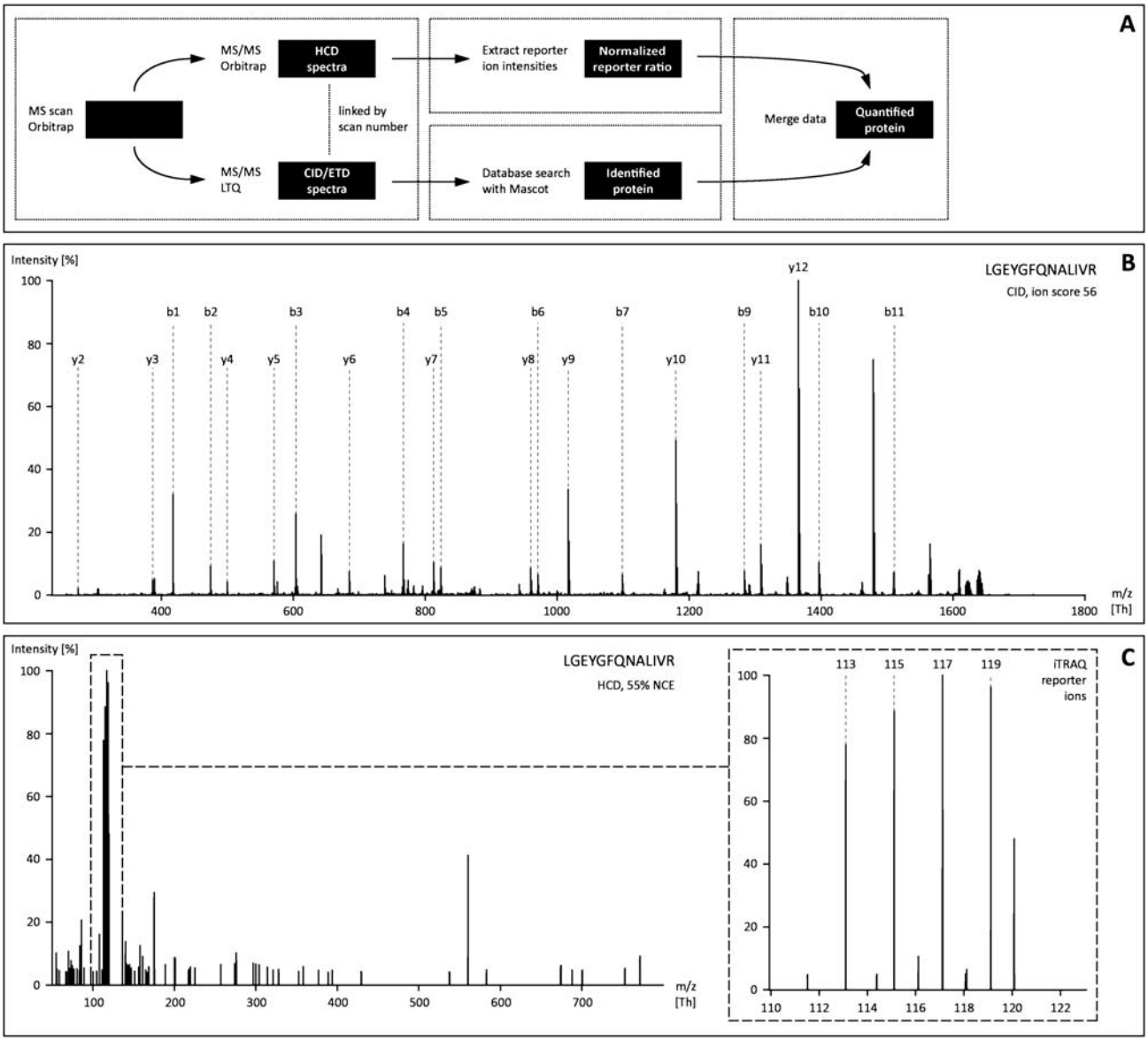

Fig. 1 Workflow diagram and illustrative HCD and CID fragment ion spectra of the BSA derived peptide LGEYGFQNALIVR. (A) Workflow depicting how a precursor selected for fragmentation from the MS scan is fragmented by both HCD and CID/ETD and how sequence-informative and quantitative information is processed separately. (B) CID spectrum with the main fragment ion series annotated. The spectrum is used exclusively for identification of the peptide and is acquired during the acquisition of the HCD spectrum of the same precursor, which is shown in panel (C) with iTRAQ reporter ions magnified in the inset. The HCD spectrum is acquired in the orbitrap with an effective FWHM resolution greater than 16 000 around *m/z* 100, allowing discriminating reporter ions against contaminations, as shown in the inset.

comparison also by offline LC followed by MALDI MS analysis on the 4800 Proteomics Analyzer.

Data processing was performed using the iTRAQ analysis platform described in the Materials and methods section. This software, which had initially been developed for iTRAQ data acquired on the 4800 Proteomics Analyzer, was adapted to handle HCD data as well. The software was linked to a Mascot-based platform for peptide identification. In the first round of data processing, proteins were identified based on the peptide sequence matches generated by Mascot (peptide ion score > peptide homology threshold established at $p < 0.01$) using relatively strict criteria, namely at least two unique peptides were required per protein and these peptides could not be assigned to any other protein. Using these criteria, these peptides were called identified peptides. In the second round of data processing, proteins were quantified using a nearly identical repetition of the first round, with two changes. The major adaptation was that the peptide ion score was not required to be bigger than the peptide homology threshold, which effectively yields a larger number of peptides. The minor adaptation was that in the HCD spectrum, which accompanied every CID or ETD spectrum and which was used to read out reporter ion intensities, the reporter ion intensities were required to be greater than 5000. Using these criteria, the peptides that could be quantified and assigned to a protein were called quantified peptides. Finally, the identified peptide pool was used to create a list of proteins, which were then

A

NCE	Reporter ion intensities 1:1:1:1			
	113	115	117	119
35	0.80 ± 0.10	1.02 ± 0.16	1.14 ± 0.10	1.10 ± 0.07
45	0.79 ± 0.07	0.99 ± 0.08	1.17 ± 0.08	1.11 ± 0.10
55	0.78 ± 0.11	1.01 ± 0.09	1.19 ± 0.23	1.11 ± 0.11
65	0.76 ± 0.06	0.96 ± 0.06	1.21 ± 0.11	1.15 ± 0.09

B

NCE	Reporter ion intensities 1:1:2:4			
	113	115	117	119
35	0.48 ± 0.05	0.58 ± 0.02	1.36 ± 0.07	2.65 ± 0.07
45	0.45 ± 0.08	0.58 ± 0.08	1.46 ± 0.20	2.75 ± 0.32
55	0.46 ± 0.08	0.58 ± 0.05	1.39 ± 0.19	2.79 ± 0.28
65	0.46 ± 0.07	0.55 ± 0.08	1.45 ± 0.15	2.83 ± 0.24

C

NCE	Reporter ion Ratios 1:1:1:1			
	113/113	115/113	117/113	119/113
35	1.00 ± 0.15	1.28 ± 0.19	1.42 ± 0.14	1.37 ± 0.12
45	1.00 ± 0.09	1.25 ± 0.11	1.48 ± 0.11	1.40 ± 0.12
55	1.00 ± 0.16	1.30 ± 0.14	1.52 ± 0.26	1.42 ± 0.16
65	1.00 ± 0.09	1.26 ± 0.09	1.59 ± 0.13	1.52 ± 0.11

D

NCE	Reporter ion Ratios 1:1:2:4			
	113/113	115/115	117/113	119/113
35	1.00 ± 0.06	1.20 ± 0.05	2.83 ± 0.09	5.50 ± 0.08
45	1.00 ± 0.11	1.30 ± 0.11	3.28 ± 0.21	6.16 ± 0.33
55	1.00 ± 0.12	1.28 ± 0.10	3.06 ± 0.21	6.13 ± 0.29
65	1.00 ± 0.10	1.21 ± 0.11	3.18 ± 0.17	6.22 ± 0.25

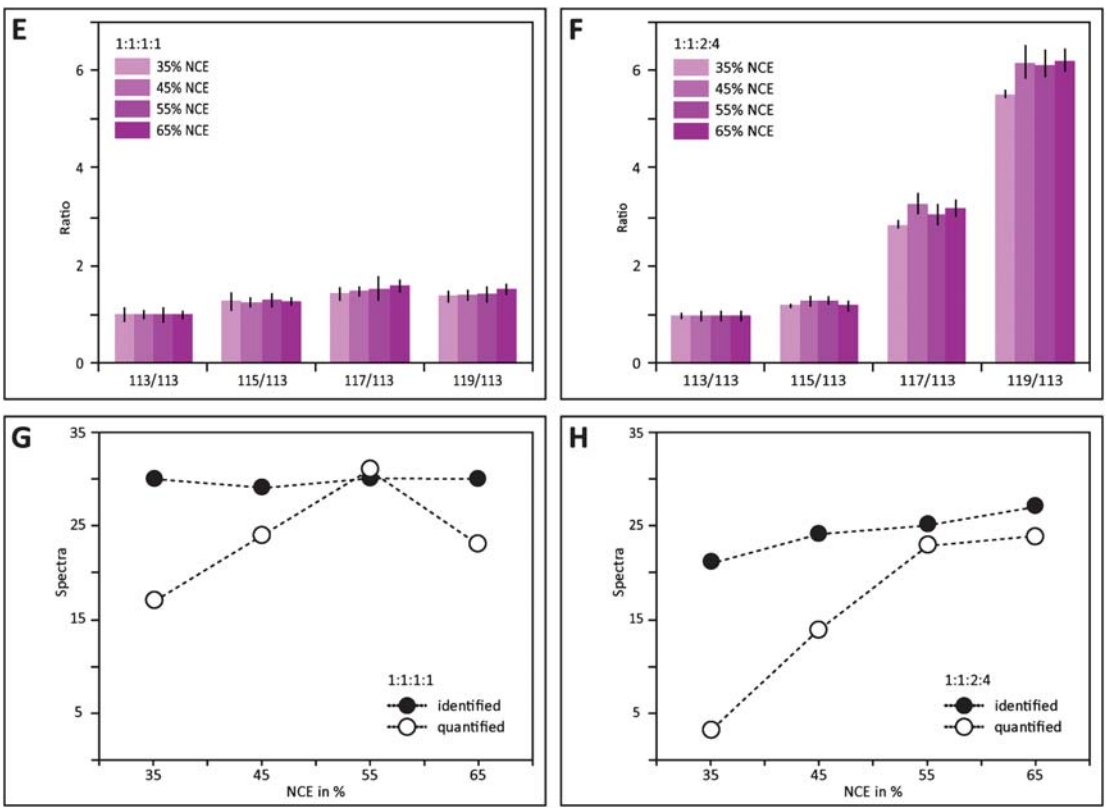

Fig. 2 Effect of HCD collision energy on the performance and accuracy of quantification. Shown here is the application of the HCD CID workflow on the quantification of 4-plex iTRAQ labeled BSA digest, mixed in ratios 1 : 1 : 1 : 1 (panels on the left) and 1 : 1 : 2 : 4 (panels on the right) at different HCD collision energies. (A and B) Normalized reporter ion intensities. At both mixing ratios of 1 : 1 : 1 : 1 and 1 : 1 : 2 : 4, each reporter ion channel has an uncertainty of around 10% which is independent of HCD collision energy. (C and D) Normalized reporter ion intensities relative to the normalized intensity of the 113 channel. The uncertainty is similar as for single channels. Note that the measured mixing ratios deviate from the nominal mixing ratios of 1 : 1 : 1 : 1 (observed as 1 : 1.3 : 1.5 : 1.4) and 1 : 1 : 2 : 4 (observed as 1 : 1.2 : 3.1 : 6) due to experimental variation. (E and F) Graphical representation of values in (C) and (D). (G and H) Number of identified and quantified BSA-derived peptides for both mixing ratios. Both graphs show how the number of quantifiable peptides increases with increasing NCE, at a relatively constant number of identified peptides.

quantified using the quantified peptide pool. The rationale behind this data analysis strategy was to achieve very strict protein identifications, but once a protein was identified to gather as much quantitative information as possible by using more relaxed criteria for selecting peptides for quantification. This procedure implies that the number of quantifiable peptides is potentially larger than the number identifiable peptides.

In our analysis we confidently identified 2907 peptides by MALDI, 3800 peptides by the HCD CID method, and 4592 peptides by the HCD CID/ETD method. Fig. 3A shows that for any of the three analyses, around 40% of the identified peptides were unique in a single analysis, and around 1000 peptides were identified by all three methods. It also shows that HCD CID/ETD identified most peptides which were not identified by the

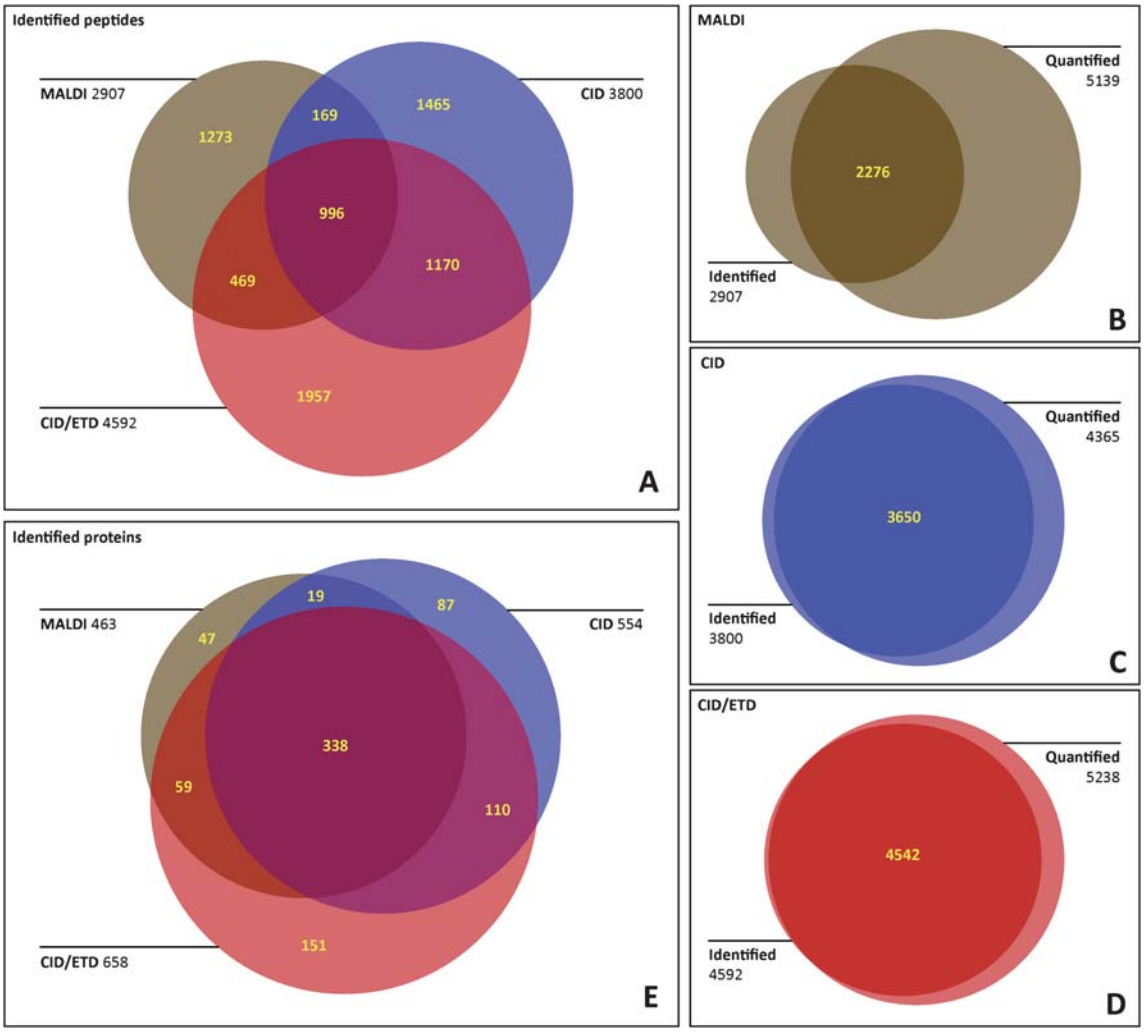

Fig. 3 Overlap between identified peptides and proteins of all three analyses and comparison of quantification efficiency. (A) Identified peptides. The Venn diagram gives an overview of peptide identifications in the MALDI, HCD CID, and HCD CID/ETD analyses, as well as their overlap. (B) Overlap between identified and quantified peptides in the MALDI analyses. Because slightly different criteria were applied to select peptides for quantification (in brief, by introducing an iTRAQ reporter ion intensity cut-off, and by dropping the homology threshold criterion for peptide matches, see Materials and methods for details), the number of quantified peptides differs from the number of identified peptides. The overlap between identified and quantified peptides, relative to the number of identified peptides, is the efficiency of quantification, which is around 80%. (C and D) Similar as in (B), but now for the HCD CID and HCD CID/ETD analyses, respectively. In both analyses, nearly all peptides that were identified from a CID or ETD spectrum could also be quantified from their corresponding HCD spectrum. Thus, the quantification efficiency is approaching 100% for these methods. (E) Identified proteins. Similar as in (A), but now for identified proteins. Clearly, at the protein level, the overlap between the three different methods is much larger than at the peptide level.

other analyses. One of the advantages of the HCD CID and even more so the HCD CID/ETD experiment over the MALDI experiment is the possibility to identify peptides in the later SCX fractions. Where the MALDI analysis does not add identifications after SCX fraction 23, because of the size and properties of the peptides, especially our HCD CID/ETD approach identified peptides up to SCX fraction 27, which consisted mainly of peptides with 4, 5 and more charges. Fig. 3B, C and D show the overlap between quantified and identified peptides for all three experiments. As can be seen from Fig. 3B, for the MALDI method around 80% of the peptides (2276), which fit the identification criteria could also be quantified, as compared to more than 95% of the peptides for both the HCD CID (3650) and the HCD CID/ETD (4542) methods (Fig. 3C and D), showing a higher efficiency in quantification for the latter two methods.

At the level of protein identification, the overlap between the three analyses is much greater (Fig. 3E), where 463 (by MALDI), 554 (by HCD CID) and 658 (by HCD CID/ETD) proteins were identified, with 338 proteins found in all three analyses. For nearly all identified proteins quantitative information could be inferred, with only 11 proteins not quantifiable by MALDI and 1 protein not quantifiable with HCD CID (Table S1†). Although the majority of proteins detected in the arbitrarily selected combinations of brain samples were found to be equally abundant, we identified a relatively small number of proteins (*i.e.* 72 by MALDI, 55 by HCD CID, and 115 by HCD CID/ETD) with

a significantly different abundance ($p < 0.01$, Fig. 4A). We used these data to investigate whether the three methods used here gave comparable quantitative results. To compare proteins found to be significantly different in two analyses, the log-ratios of two arbitrarily selected label combinations, namely 114 : 116 and 118 : 121, were compared pair wise (Fig. 4B, C and D). These ratios correlate very well, both when comparing HCD CID to HCD CID/ETD (Fig. 4B) and when comparing either of the two orbitrap analyses to the MALDI TOF/TOF analysis (Fig. 4C and D). In all three cases, the correlation coefficient was around 0.95.

From our protein identification data we can conclude, as expected, that the human synapse proteome resembles the rodent synapse proteome.[34] Proteins that are known to be present in the pre-synaptic terminal and post-synaptic compartment were well represented in our data, including synaptic vesicle proteins, adhesion molecules, scaffolding proteins, receptors, ion channels, signaling proteins and proteins involved in trafficking. Mitochondrial proteins, metabolic proteins and structural proteins that are commonly observed in rodent synapse proteomes were also detected. Furthermore, the observed protein expression profiles between the four human brain samples were very comparable with only a low number of proteins (around 10%) showing significant differences between samples, mainly clustered around a logarithmic ratio of 0.5 and a maximum at 1.5. These results indicate that the brain biopsies as used here in this study might be valuable control samples in future studies of human brain disease. Protein and peptide identifications can be found in the ESI†.

To conclude, we present here a workflow that allows quantitative analysis of iTRAQ labeled peptides by parallel peptide quantification and peptide identification. The workflow is easily

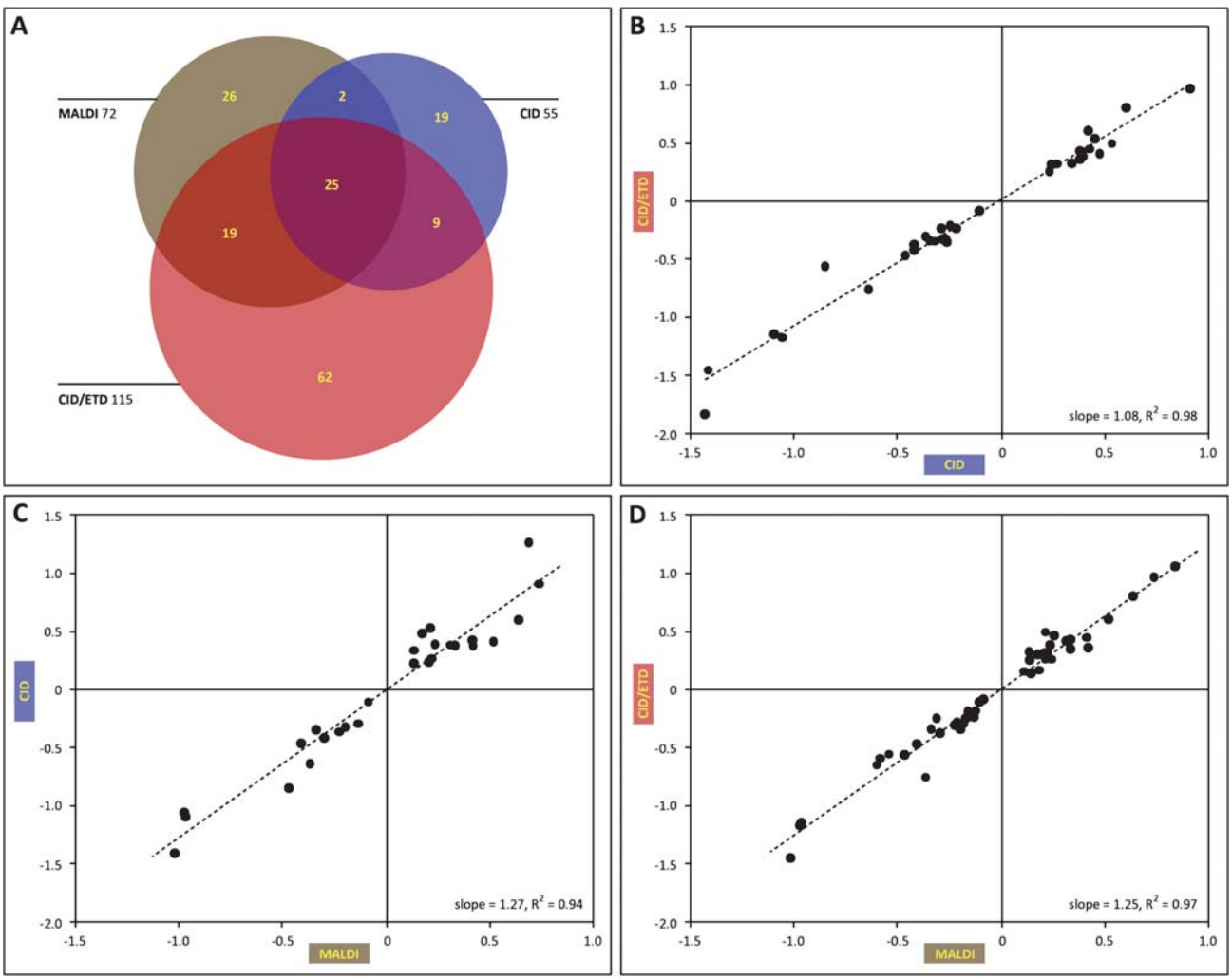

Fig. 4 Differential protein abundances and their comparison between the three analyses. (A) Number of proteins with differential abundance between selected samples. The Venn diagram shows proteins found to be differentially abundant (with a significance threshold below 0.01) when comparing the arbitrarily chosen channels 114 *versus* 116 and 118 *versus* 121. (B–D) Comparison of protein abundances expressed in log-ratios detected by two methods. Each dot in a diagram represents the logarithmic ratios 114/116 or 118/121 of a single protein found to be significantly differentially abundant in two of the three analyses, which can be either HCD CID/ETD *versus* HCD CID (B), HCD CID *versus* MALDI (C), or HCD CID/ETD *versus* MALDI (D). In all three diagrams, a very strong linear correlation can be observed, which means that the three methods give very similar protein quantification results.

set up on a HCD-enabled LTQ Orbitrap and allows decision-tree guided ETD for peptide identification. We show that by combining CID and ETD using the decision tree, we can outperform a MALDI TOF/TOF instrument in terms of peptide and protein identification as well as protein quantification. Utilizing HCD solely for the determination of the iTRAQ reporter ions circumvents long ion accumulation times, generates the same iTRAQ reporter ions in both CID and ETD peptide identification events and leads to very high quantification efficiency. Finally, we demonstrate that our workflow is applicable to the quantitative analysis of the synapse proteomes from *postmortem* human brains. In principle, this method can also be used to quantitatively characterize the human synapse proteome isolated from patients with brain disorders, which should give insights into the molecular mechanisms of these disorders.

Abbreviations

MS	mass spectrometry
SILAC	stable isotope labeling by amino acids in cell culture
ICAT	isotope-coded affinity tagging
iTRAQ	isobaric tagging for relative and absolute quantification
MS/MS	tandem mass spectrometry
PQD	pulsed Q collision induced dissociation
HCD	higher energy collisional dissociation
CID	collision induced dissociation
MALDI	matrix assisted laser desorption ionization
TOF	time of flight
ETD	electron transfer dissociation
BSA	bovine serum albumin
SCX	strong cation exchange
LC	liquid chromatography
ID	inner diameter
OD	outer diameter
AGC	automatic gain control
NCE	normalized collision energy
FWHM	full width at half maximum

Acknowledgements

The authors wish to thank Dr Shabaz Mohammed for critical discussion and Patricia Klemmer for the preparation of iTRAQ labeled samples. ABS and KWL are supported by grants of the Center for Medical Systems Biology. NM and AJRH are supported by the NGI Horizon Program grant number 050-71-050, and NM, AJRH and AFMA additionally by the Netherlands Proteomics Centre.

References

1 R. Aebersold and M. Mann, Mass spectrometry-based proteomics, *Nature*, 2003, **422**, 198–207.
2 A. J. Heck and J. Krijgsveld, Mass spectrometry-based quantitative proteomics, *Expert Rev. Proteomics*, 2004, **1**, 317–326.
3 S. E. Ong, B. Blagoev, I. Kratchmarova, D. B. Kristensen, H. Steen, A. Pandey and M. Mann, Stable isotope labeling by amino acids in cell culture, SILAC, as a simple and accurate approach to expression proteomics, *Mol. Cell. Proteomics*, 2002, **1**, 376–386.
4 Y. Oda, K. Huang, F. R. Cross, D. Cowburn and B. T. Chait, Accurate quantitation of protein expression and site-specific phosphorylation, *Proc. Natl. Acad. Sci. U. S. A.*, 1999, **96**, 6591–6596.
5 J. Krijgsveld, R. F. Ketting, T. Mahmoudi, J. Johansen, M. Artal-Sanz, C. P. Verrijzer, R. H. Plasterk and A. J. Heck, Metabolic labeling of *C. elegans* and *D. melanogaster* for quantitative proteomics, *Nat. Biotechnol.*, 2003, **21**, 927–931.
6 C. C. Wu, M. J. MacCoss, K. E. Howell, D. E. Matthews and J. R. Yates, 3rd, Metabolic labeling of mammalian organisms with stable isotopes for quantitative proteomic analysis, *Anal. Chem.*, 2004, **76**, 4951–4959.
7 M. Kruger, M. Moser, S. Ussar, I. Thievessen, C. A. Luber, F. Forner, S. Schmidt, S. Zanivan, R. Fassler and M. Mann, SILAC mouse for quantitative proteomics uncovers kindlin-3 as an essential factor for red blood cell function, *Cell*, 2008, **134**, 353–364.
8 S. P. Gygi, B. Rist, S. A. Gerber, F. Turecek, M. H. Gelb and R. Aebersold, Quantitative analysis of complex protein mixtures using isotope-coded affinity tags, *Nat. Biotechnol.*, 1999, **17**, 994–999.
9 P. L. Ross, Y. N. Huang, J. N. Marchese, B. Williamson, K. Parker, S. Hattan, N. Khainovski, S. Pillai, S. Dey, S. Daniels, S. Purkayastha, P. Juhasz, S. Martin, M. Bartlet-Jones, F. He, A. Jacobson and D. J. Pappin, Multiplexed protein quantitation in *Saccharomyces cerevisiae* using amine-reactive isobaric tagging reagents, *Mol. Cell. Proteomics*, 2004, **3**, 1154–1169.
10 P. J. Boersema, T. T. Aye, T. A. van Veen, A. J. Heck and S. Mohammed, Triplex protein quantification based on stable isotope labeling by peptide dimethylation applied to cell and tissue lysates, *Proteomics*, 2008, **8**, 4624–4632.
11 P. J. Boersema, R. Raijmakers, S. Lemeer, S. Mohammed and A. J. Heck, Multiplex peptide stable isotope dimethyl labeling for quantitative proteomics, *Nat. Protoc.*, 2009, **4**, 484–494.
12 D. L. Meany, H. Xie, L. V. Thompson, E. A. Arriaga and T. J. Griffin, Identification of carbonylated proteins from enriched rat skeletal muscle mitochondria using affinity chromatography-stable isotope labeling and tandem mass spectrometry, *Proteomics*, 2007, **7**, 1150–1163.
13 M. Hardman and A. A. Makarov, Interfacing the orbitrap mass analyzer to an electrospray ion source, *Anal. Chem.*, 2003, **75**, 1699–1705.
14 J. C. Schwartz, J. P. Syka, and S. T. Quarmby, *53rd ASMS Conference on Mass Spectrometry*, San Antonio, Texas, 2005.
15 J. V. Olsen, B. Macek, O. Lange, A. Makarov, S. Horning and M. Mann, Higher-energy C-trap dissociation for peptide modification analysis, *Nat. Methods*, 2007, **4**, 709–712.
16 T. J. Griffin, H. Xie, S. Bandhakavi, J. Popko, A. Mohan, J. V. Carlis and L. Higgins, iTRAQ reagent-based quantitative proteomic analysis on a linear ion trap mass spectrometer, *J. Proteome Res.*, 2007, **6**, 4200–4209.
17 M. Bantscheff, M. Boesche, D. Eberhard, T. Matthieson, G. Sweetman and B. Kuster, Robust and sensitive iTRAQ quantification on an LTQ orbitrap mass spectrometer, *Mol. Cell. Proteomics*, 2008, **7**, 1702–1713.
18 Y. Zhang, S. B. Ficarro, S. Li and J. A. Marto, Optimized orbitrap HCD for quantitative analysis of phosphopeptides, *J. Am. Soc. Mass Spectrom.*, 2009, **20**(8), 1425–34.
19 T. Kocher, P. Pichler, M. Schutzbier, C. Stingl, A. Kaul, G. Hasenfuss, N. Teucher, J. Penninger and K. Mechtler, High precision quantitative proteomics using iTRAQ on an LTQ orbitrap: a new mass spectrometric method combining the benefits of all, *J. Proteome Res.*, 2009, **8**(10), 4743–52.
20 M. M. Savitski, F. Fischer, T. Mathieson, G. Sweetman, M. Lang, and M. Bantscheff, Targeted data acquisition for improved reproducibility and robustness of proteomic mass spectrometry assays, *J. Am. Soc. Mass Spectrom.*, DOI: 10.1016/j.jasms.2010.01.012.
21 L. Dayon, C. Pasquarello, C. Hoogland, J.-C. Sanchez and A. Scherl, Combining low- and high-energy tandem mass spectra for optimized peptide quantification with isobaric tags, *J. Proteomics*, 2010, **73**, 769–777.
22 J. J. Coon, B. Ueberheide, J. E. Syka, D. D. Dryhurst, J. Ausio, J. Shabanowitz and D. F. Hunt, Protein identification using sequential ion/ion reactions and tandem mass spectrometry, *Proc. Natl. Acad. Sci. U. S. A.*, 2005, **102**, 9463–9468.

23 S. J. Pitteri, P. A. Chrisman, J. M. Hogan and S. A. McLuckey, Electron transfer ion/ion reactions in a three-dimensional quadrupole ion trap: reactions of doubly and triply protonated peptides with SO_2*, *Anal. Chem.*, 2005, **77**, 1831–1839.

24 H. W. P. Toorn van de, S. Mohammed, J. W. Gouw, B. Breukelen van and A. J. R. Heck, Targeted SCX based peptide fractionation for optimal sequencing by collision- and electron transfer-induced dissociation, *J. Proteomics Bioinf.*, 2008, **1**, 379–388.

25 H. Molina, R. Matthiesen, K. Kandasamy and A. Pandey, Comprehensive comparison of collision induced dissociation and electron transfer dissociation, *Anal. Chem.*, 2008, **80**, 4825–4835.

26 D. L. Swaney, G. C. McAlister, M. Wirtala, J. C. Schwartz, J. E. Syka and J. J. Coon, Supplemental activation method for high-efficiency electron-transfer dissociation of doubly protonated peptide precursors, *Anal. Chem.*, 2007, **79**, 477–485.

27 H. Han, D. J. Pappin, P. L. Ross and S. A. McLuckey, Electron transfer dissociation of iTRAQ labeled peptide ions, *J. Proteome Res.*, 2008, **7**, 3643–3648.

28 D. Phanstiel, Y. Zhang, J. A. Marto and J. J. Coon, Peptide and protein quantification using iTRAQ with electron transfer dissociation, *J. Am. Soc. Mass Spectrom.*, 2008, **19**, 1255–1262.

29 D. Phanstiel, R. Unwin, G. C. McAlister and J. J. Coon, Peptide quantification using 8-plex isobaric tags and electron transfer dissociation tandem mass spectrometry, *Anal. Chem.*, 2009, **81**, 1693–1698.

30 F. Yang, S. Wu, D. L. Stenoien, R. Zhao, M. E. Monroe, M. A. Gritsenko, S. O. Purvine, A. D. Polpitiya, N. Tolic, Q. Zhang, A. D. Norbeck, D. J. Orton, R. J. Moore, K. Tang, G. A. Anderson, L. Pasa-Tolic, D. G. Camp and R. D. Smith, Combinedpulsed-Q dissociation and electron transfer dissociation for identification and quantification of iTRAQ-labeled phosphopeptides, *Anal. Chem.*, 2009, **81**(10), 4137–43.

31 D. L. Swaney, G. C. McAlister and J. J. Coon, Decision tree-driven tandem mass spectrometry for shotgun proteomics, *Nat. Methods*, 2008, **5**, 959–964.

32 M. A. Kuzyk, L. B. Ohlund, M. H. Elliott, D. Smith, H. Qian, A. Delaney, C. L. Hunter and C. H. Borchers, A comparison of MS/MS-based, stable-isotope-labeled, quantitation performance on ESI-quadrupole TOF and MALDI-TOF/TOF mass spectrometers, *Proteomics*, 2009, **9**, 3328–3340.

33 K. H. Smalla, M. Mikhaylova, J. Sahin, H. G. Bernstein, B. Bogerts, A. Schmitt, R. van der Schors, A. B. Smit, K. W. Li, E. D. Gundelfinger and M. R. Kreutz, A comparison of the synaptic proteome in human chronic schizophrenia and rat ketamine psychosis suggest that prohibitin is involved in the synaptic pathology of schizophrenia, *Mol. Psychiatry*, 2008, **13**, 878–896.

34 K. W. Li, S. Miller, O. Klychnikov, M. Loos, J. Stahl-Zeng, S. Spijker, M. Mayford and A. B. Smit, Quantitative proteomics and protein network analysis of hippocampal synapses of CaMKIIalpha mutant mice, *J. Proteome Res.*, 2007, **6**, 3127–3133.

35 S. Y. Ow, M. Salim, J. Noirel, C. Evans, I. Rehman and P. C. Wright, iTRAQ underestimation in simple and complex mixtures: "The good, the Bad and the Ugly", *J. Proteome Res.*, 2009, **8**(11), 5347–55.

36 N. Taouatas, A. F. Altelaar, M. M. Drugan, A. O. Helbig, S. Mohammed and A. J. Heck, Strong cation exchange-based fractionation of Lys-N-generated peptides facilitates the targeted analysis of post-translational modifications, *Mol. Cell. Proteomics*, 2009, **8**, 190–200.

